

Effects of wind-powered hydrogen fuel cell vehicles on stratospheric ozone and global climate

Mark Z. Jacobson¹

Received 23 June 2008; revised 12 August 2008; accepted 20 August 2008; published 2 October 2008.

[1] Converting the world's fossil-fuel onroad vehicles (FFOV) to hydrogen fuel cell vehicles (HFCV), where the H_2 is produced by wind-powered electrolysis, is estimated to reduce global fossil, biofuel, and biomass-burning emissions of CO_2 by $\sim 13.4\%$, NO_x $\sim 23.0\%$, nonmethane organic gases $\sim 18.9\%$, black carbon $\sim 8\%$, H_2 $\sim 3.2\%$ (at 3% leakage), and H_2O $\sim 0.2\%$. Over 10 years, such reductions were calculated to reduce tropospheric CO $\sim 5\%$, NO_x $\sim 5\text{--}13\%$, most organic gases $\sim 3\text{--}15\%$, OH $\sim 4\%$, ozone $\sim 6\%$, and PAN $\sim 13\%$, but to increase tropospheric CH_4 $\sim 0.25\%$ due to the lower OH . Lower OH also increased upper tropospheric/lower stratospheric ozone, increasing its global column by $\sim 0.41\%$. WHFCV cooled the troposphere and warmed the stratosphere, reduced aerosol and cloud surface areas, and increased precipitation. Other renewable-powered HFCV or battery electric vehicles should have similar impacts. **Citation:** Jacobson, M. Z. (2008), Effects of wind-powered hydrogen fuel cell vehicles on stratospheric ozone and global climate, *Geophys. Res. Lett.*, 35, L19803, doi:10.1029/2008GL035102.

1. Introduction

[2] Several studies have examined the effects of replacing fossil-fuel onroad vehicles (FFOV) with hydrogen fuel cell vehicles (HFCV). *Tromp et al.* [2003] suggested with a 2-D model that H_2 leaks from HFCV might increase water vapor and cool the stratosphere, delaying ozone-layer recovery. The paper did not consider the simultaneous reduction in fossil-fuel emissions. *Schultz et al.* [2003] calculated that leaked H_2 and lower NO_x and CO from a hydrogen economy might decrease OH and increase CH_4 in the troposphere. *Warwick et al.* [2004] examined the effect of H_2 leaks and reduced NO_x , CO , CH_4 , and NMHC on tropospheric/stratospheric chemistry with a 2-D model. None of these studies examined aerosol particle changes or their cloud feedbacks. *Jacobson et al.* [2005] and *Colella et al.* [2005] treated such feedbacks but examined only surface air pollution and climate-relevant emission changes from converting U.S. onroad vehicles to HFCV, where the H_2 originated from natural gas steam reforming, wind electrolysis, or coal gasification. All three methods reduced pollution, but electrolysis reduced climate emissions most.

[3] To date, no study has examined the effect on stratospheric ozone or global climate of converting from FFOV to HFCV while treating particle and gas emission changes from both. Here, a 3-D model is used to examine these

issues when the H_2 for HFCV is generated by wind electrolysis (hereinafter WHFCV). Wind electrolysis is considered because it emits fewer air pollutants and greenhouse gases than does steam-reforming or coal gasification [*Colella et al.*, 2005]. As such, the effects of FFOV and WHFCV bound the impacts of HFCV. Although a 100% conversion to WHFCV is unlikely, it gives the upper limit of effects. Results for other penetrations can be scaled accordingly.

2. Model and Simulation Description

[4] The model used was GATOR-GCMOM, which solves dynamical, gas, aerosol, cloud, transport, radiation, and surface processes [*Jacobson*, 2001, 2006; *Jacobson et al.*, 2007]. Simulations were run on a $4^\circ\text{S-N} \times 5^\circ\text{W-E}$ global domain with 49 layers up to 0.22 hPa (≈ 60 km). Two 10-year simulations were run: one with contemporary FFOV emissions ("baseline" scenario) and another with WHFCV emissions ("WHFCV scenario"). WHFCV were assumed to emit only water vapor and hydrogen. The auxiliary material¹ (AM) describes the model and emission scenarios. Tables 1 and S3 respectively summarize gas and particle emission changes. Replacing FFOV with WHFCV reduced global fossil, biofuel, and biomass-burning emissions of CO $\sim 20.6\%$, CO_2 $\sim 13.4\%$, NO_x $\sim 23.0\%$, N_2O $\sim 0.8\%$, SO_x $\sim 2.8\%$, CH_4 $\sim 0.25\%$, nonmethane organic gases (NMOG) $\sim 18.9\%$, BC $\sim 8.0\%$, and primary organic matter (POM) $\sim 1.5\%$. Whereas 3% H_2 leakage associated with WHFCV increased H_2 emissions, the elimination of FFOV, which emitted 0.0285 g- H_2 /g-CO [*Barnes et al.*, 2003] reduced H_2 emissions more (AM). H_2O increases due to WHFCV also effectively offset H_2O decreases from eliminating FFOV (AM). The small net H_2 and H_2O emission changes are not statistically significant.

[5] The model treated two aerosol size distributions (14 size bins each) and three hydrometeor distributions (liquid, ice, graupel - 30 bins each) (Table S1). Twenty aerosol, liquid, ice, and graupel heterogeneous chemical reactions were solved together with 314 kinetic and 57 photolysis reactions (391 total; see AM) with SMVGear II. A new method of converting pseudo-first-order to second-order rate coefficients to ensure mass conservation of heterogeneous reactions was developed (AM, equation (S8)).

3. Results

[6] The AM discusses previous evaluations of the model. Figure 1 additionally compares monthly vertical ozone,

¹Department of Civil and Environmental Engineering, Stanford University, Stanford, California, USA.

Table 1. Global Gas Emissions^a

Species	FFOV (Tg/yr)	WHFCV (Tg/yr)	Biomass Burning (Tg/yr)	Biofuel Burning (Tg/yr)	Other Anthropogenic Sources (Tg/yr)	All Base Anthropogenic Sources ^b (Tg/yr)	All WHFCV Anthropogenic Sources ^c (Tg/yr)	Natural Sources (Tg/yr)
<i>Inorganic Gases</i>								
Carbon monoxide	195.7	0	420	216	119.1	950.8	755.1	0.003 ^a
Carbon dioxide	3760	0	3200 ^d	170 ^d	21,010	28,140	24,380	
Nitric oxide	16	0	14	2.7	37	69.7	53.7	25.4
Nitrogen dioxide	2.75	0	2.2	0.42	6.35	11.7	8.97	1.3
Nitrous acid	0.224	0	0.25	0.048	0.523	1.05	0.821	0.12
Nitrous oxide	0.10	0	1.1	0.17	11.02	12.4	12.3	10.1
Sulfur dioxide	4.0	0	2.5	0.72	136.2	143.4	139.4	9.7
Sulfur trioxide	0.14	0	0.078	0.022	5.34	5.58	5.44	0
Sulfuric acid	0.06	0	0.026	0.0074	2.18	2.27	2.21	0
Ammonia	0	0	6.0	3.6	45.18	54.8	54.8	13.0
Molec. hydrogen	5.58	4.82	9.8	5.0	3.38	23.8	23	7.0
Water vapor	1420	1390	2770	1460	9590	15,240	15,210	^a
<i>Organic Gases</i>								
Methane	0.8	0	19.7	20.2	275.9	317	316	221
Paraffin group	14.7	0	7.0	7.3	38.0	67	52.3	260
Ethene	1.83	0	6.0	5.0	2.54	15.4	13.5	0
Olefin group	2.10	0	2.2	4.1	2.75	11.2	9.1	13
Methanol	1.85	0	8.3	4.2	2.65	17.0	15.2	310
Formaldehyde	0.41	0	4.9	0.36	0.57	6.24	5.83	0
Higher aldehydes	1.20	0	2.8	0.39	1.67	6.06	4.86	0
Benzene	1.04	0	1.6	5.3	1.47	9.41	8.37	0
Toluene group	1.96	0	1.0	3.0	2.67	8.63	6.67	0
Xylene group	2.77	0	0.36	1.5	3.69	8.32	5.55	0
Total organic gas ^e	28.7	0	53.9	51.4	331.1	465	436	804

^aThe AM describes the data sources and method of calculating emissions in each scenario. Biomass burning is ~90% anthropogenic and ~10% natural, but 100% is included in the seventh and eighth columns. Natural emission sources of CO₂ and H₂O dwarf anthropogenic sources and have nearly equally-large sinks so are not included in the table.

^bIncludes FFOV, biomass burning, biofuel burning, and other sources.

^cIncludes WHFCV, biomass burning, biofuel burning, and other sources.

^dBiomass- and biofuel-burning CO₂ emissions are burning minus regrowth during year.

^eIsoprene (530 Tg-C/yr), monoterpenes (144 Tg-C/yr), dimethylsulfide (31.8 Tg/yr), and some other organics were included in the simulations but are not shown in the table.

temperature, and dew point profiles with model values in the same locations as the measurements. The comparisons indicate extremely good agreement considering the coarseness of the model resolution.

[7] WHFCV decreased the ambient global column of the vehicle-emitted chemicals, H₂, CO₂, NO, NO₂, CO, HCHO, CH₃CHO, benzene, toluene, black carbon (BC), and primary organic matter (POM) (Table S2 and Figures S1a–S1k) in the same direction as their emission reductions. WHFCV also decreased column secondary organic matter (SOM), S(VI), HNO₃, and NO₃[−] by 6%, 3%, 2%, and 19%, respectively (Table S2 and Figures S1l–S1o) due to reductions in aerosol-precursor gases.

[8] The decrease in tropospheric ozone precursors due to WHFCV decreased surface ozone by ~1 ppbv globally and up to 5 ppbv regionally (Figure 2a and Table S2), a result expected from studies that have examined the impact of fossil-fuel vehicle emissions on surface ozone [e.g., Granier and Brasseur, 2003]. WHFCV, though, increased column ozone by ~0.41% (Table S2), by increasing upper-tropospheric/lower-stratospheric (UTLS) ozone. UTLS ozone increased between 200–50 hPa, peaking at 80 hPa, primarily in the Northern Hemisphere (Figure 2a). The increase correlates very well with an up to 4% OH decrease in the same region (Figure S1p). Since HO_x is the main family to destroy UTLS ozone, OH reductions should increase ozone there. OH is produced by NO + HO₂, HONO + hν, and O(¹D) + H₂O. WHFCV reduced column NO by 9%, column HCHO and

CH₃CHO (which produce HO₂) by 3.9 and 1.6%, respectively (Table S2), column HONO, and tropospheric O(¹D) (by reducing tropospheric O₃ by 6%, Figure 2a). These reductions outweighed a slight (0.1%) tropospheric H₂O increase (Figure 2b), causing a net OH loss. UTLS ozone was also affected by aerosol and cloud changes, discussed shortly.

[9] Although CH₄ emissions decreased by ~0.25%, column CH₄ increased slightly (+0.25%) due to tropospheric CH₄ increases (Figure S1q) caused by OH losses (Figure S1p). Because methane's mixing ratio was not in equilibrium with its emissions reduction after 10 years (since methane's lifetime against OH loss is 8–12 years), CH₄ may change further over a longer simulation. Tropospheric OH and O₃ decreases reduced chemical loss of isoprene and monoterpenes, increasing their concentrations and reducing SOM (Table S2). The reduction in NO_x and organic gas emissions due to WHFCV decreased near-surface PAN by up to 13% (Figure S1r).

[10] WHFCV did not increase anthropogenic water vapor emissions compared with FFOV (Table 1), but did increase ambient column water vapor by about 0.22% (Table S2 and Figure 2b). The water vapor increase was due primarily to conversion of cloud liquid and ice to water vapor and precipitation (Table S2). WHFCV increased precipitation by decreasing emissions of anthropogenic cloud condensation nuclei (CCN), ice deposition nuclei (IDN) (Table S3), and their precursor gases (Table 1), reducing particle number (Figure S1s) and activated CCN and IDN (Table S2).

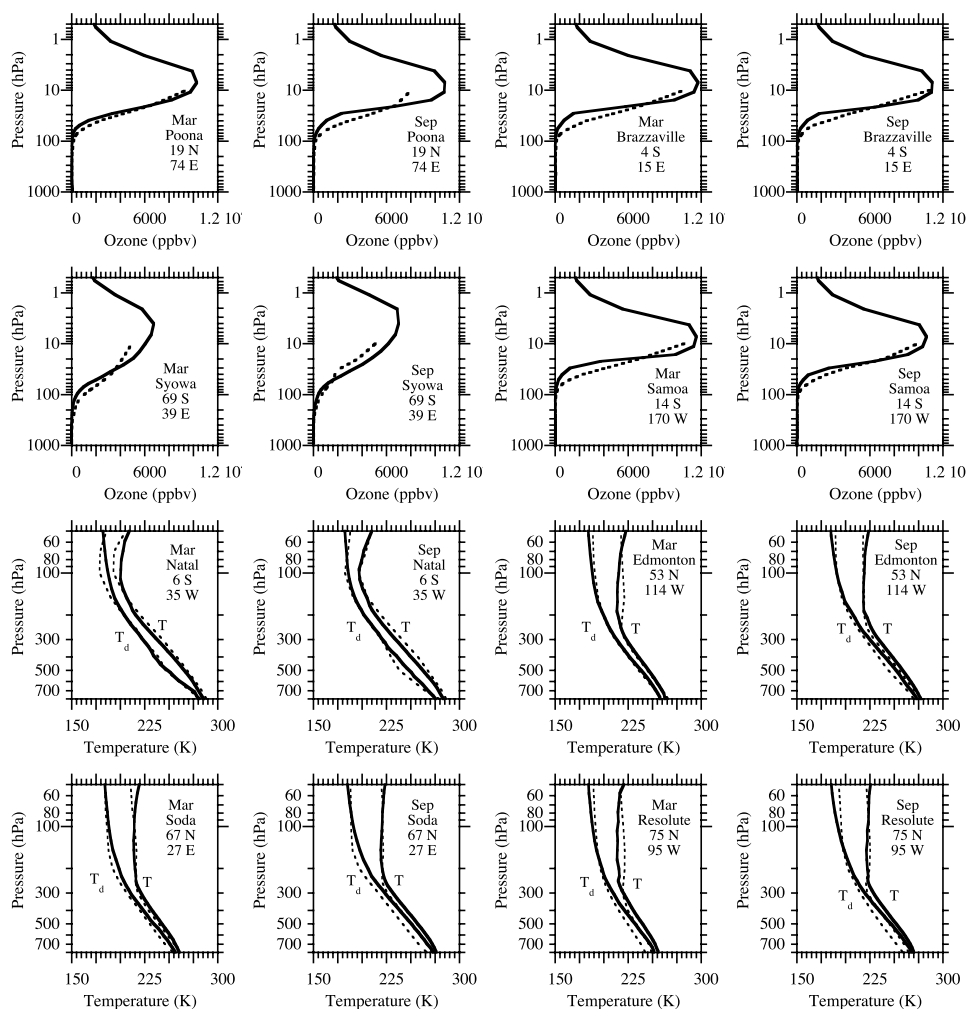


Figure 1. Comparison of monthly-averaged vertical profiles of modeled ($4^\circ \times 5^\circ$) baseline (solid lines) versus observed (dashed lines) ozone [Logan, 1999], temperature, and dew point [Forecast Systems Laboratory, 2008].

CCN and IDN decreases increased drop size, increasing precipitation, and they decreased column cloud liquid, ice (Table S2, Figure 2c, and Figure S1t), optical depth (Table S2), and fraction (Table S2), as expected from satellite correlation [Koren *et al.*, 2005]. UTLS warming (Figure 2d) contributed to the ice decrease. Natural IDN, including soil dust (Figure S1aa), pollen, spores, bacteria (Table S2), and sea-spray sodium (Figure S1y) and chloride (Figure S1z), decreased slightly due to precipitation increases and reduced surface wind speeds.

[11] Greenhouse gases (GHGs) warm the surface and cool the stratosphere, thus their removal does the reverse, but over years to decades. Aerosol particles consist of warming components (e.g., BC, some POM) and cooling components (e.g., S(VI), NO_3^- , most POM and SOM). Cooling components dominate, so overall, aerosol particles cause net surface cooling, and their removal (with WHFCV) causes surface warming over weeks to years by reducing aerosol and cloud optical depths and increasing surface solar radiation (e.g., Table S2). WHFCV decreased GHG and aerosol emissions, so the net impact depended on the period during which changes occurred. For the 10-y simulations, a slight surface cooling and stronger UTLS warming occurred (Figure 2d), which likely raised tropopause heights. UTLS warming occurred globally and was en-

hanced by the ozone increase there (Figure 2a). Over a longer simulation, the surface cooling and stratospheric warming should strengthen. Averaged over the simulation, the top-of-atmosphere irradiance change was $+0.07 \text{ W/m}^2$, due primarily to the greater reduction in cloud optical depth than CO_2 . This should decrease (and become negative) as CO_2 decreases further with a longer simulation.

[12] The increase in UTLS ozone warmed the UTLS but cooled the air above it over much of the Northern Hemisphere by reducing thermal-IR penetration from the troposphere to above the UTLS. This cooling slightly increased ice clouds (Figure 2c) and ozone loss at 25 km over the Antarctic and increased ozone loss above the UTLS globally from 22–40 km (40–2 hPa) (Figure 2a). Ozone increased in the UTLS more than it decreased above the UTLS, causing a net ozone column increase.

[13] Whereas UTLS ozone increase was due primarily to OH loss, WHFCV also increased UTLS ozone by reducing aerosol and ice cloud surface area on which ozone-destroying halogen gases could form and reducing nitric acid available for nitric acid trihydrate (NAT) ice crystals. WHFCV reduced aerosol surface area by reducing BC, POM, and S(VI) emissions and increasing precipitation. By reducing ambient S(VI), NO_3^- , and SOM, WHFCV reduced hydrated aerosol water and cloud liquid water

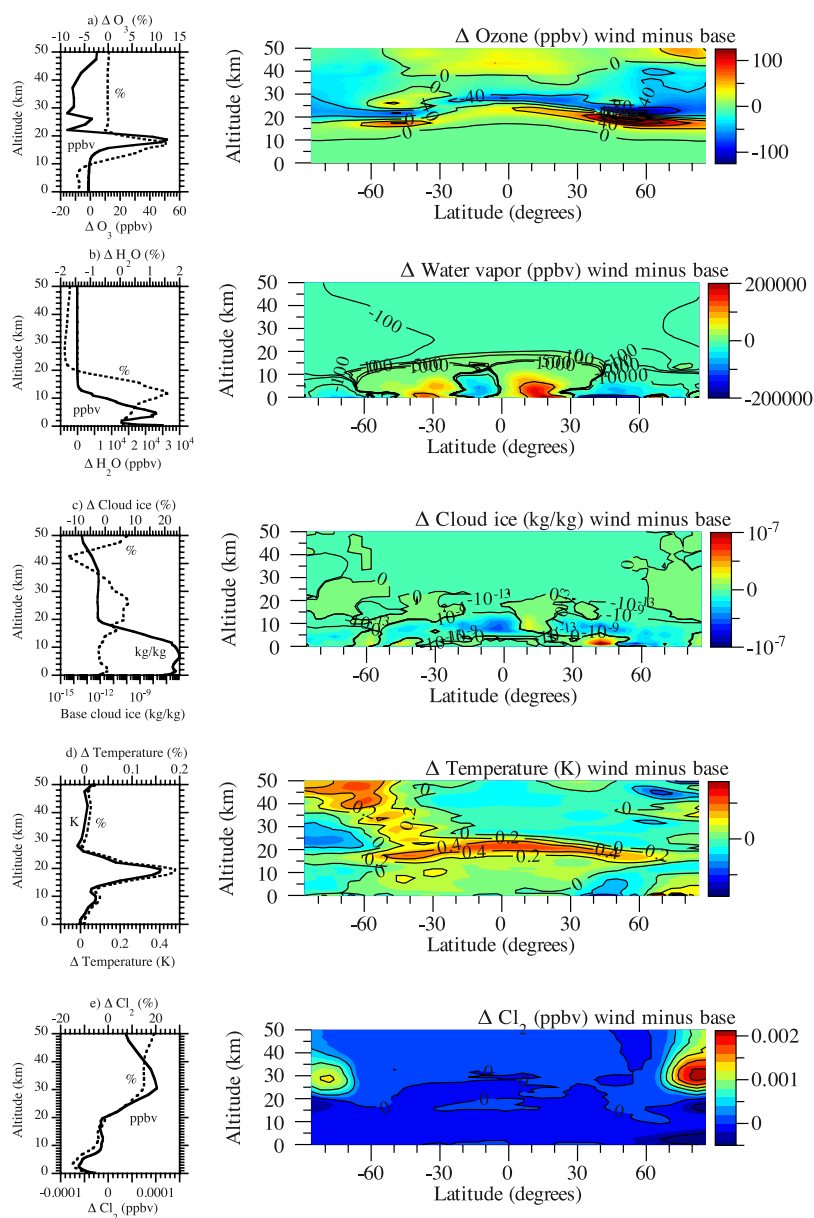


Figure 2. Modeled annually-averaged vertical profiles of (left) the globally-averaged and (right) zonally-averaged baseline values or differences between the WHFCV (“wind”) and FFOV (“base”) values. Percent changes are also shown in the left plots.

(Table S2), decreasing SO_2 , HNO_3 , and NH_3 dissolution, decreasing aerosol size further, but increasing column SO_2 by 0.89% and NH_3 by 2.8% (Table S2). In the UTLS, HNO_3 and particle nitrate decreased by up to 4% (Figure S1n) and 2% (Figure S1o), respectively, reducing the NAT surfaces on which heterogeneous reactions could occur. BC, POM, and SOM decreased in the UTLS up to 65 hPa (Figures S1j–S1l). On the other hand, S(VI) decreased up to only 150 hPa and increased above that (Figure S1m) due to the SO_2 increase in the UTLS.

[14] The reduced UTLS aerosol surface area decreased heterogeneous reactions, reducing ambient Cl_2 by up to 4% (Figure 2e) and $HOCl$ by up to 5% there (Figure S1x). The chlorine shifted to HCl and Cl^- , which increased up to 2% (Figure S1u) and 1.5% (Figure S1y), respectively. Cl^- could increase because aerosol particles contained less nitric

acid and, in some locations, sulfuric acid, which are less volatile acids than HCl . Although UTLS reactions away from the poles are less efficient than in the polar winter stratosphere where temperatures are colder, many still occur. The enhanced water ice over the Antarctic stratosphere increased Cl_2 there (Figure 2e).

[15] WHFCV increased column BrO by 3.3%, primarily in the UTLS region (Table S2 and Figure S1bb) by reducing OH and NO_x and their reactions with BrO. Because less Br formed by BrO reaction with OH, the increase in BrO did not affect ozone significantly.

4. Discussion

[16] Tromp *et al.* [2003] suggested H_2 alone added to the stratosphere might increase water vapor, delaying

ozone-layer recovery. Here, WHFCV replacing FFOV changed H_2 only slightly but it decreased aldehydes, other organics, and NO_x , reducing OH, increasing UTLS and column ozone and decreasing mid-/lower-tropospheric O_3 . Schultz *et al.* [2003] suggested that an H_2 economy might reduce tropospheric OH, increasing tropospheric CH_4 and reducing tropospheric O_3 . Those results are in the same direction as here, but did not account for aerosol or CH_4 emission reductions or stratospheric O_3 . Here, CH_4 emission reductions offset some CH_4 chemical increases, and OH losses increased UTLS and column O_3 . Warwick *et al.* [2004] found a tropospheric OH decrease and CH_4 increase as well, but ambiguous ozone results in their 2-D model,

[17] The results here were obtained assuming contemporary emissions in the FFOV case. A full hydrogen economy, though, could take decades to implement, during which, natural emissions will change, FFOV will become more efficient, and halogen mixing ratios will decline. In the last case, the increases in stratospheric ozone due to WHFCV should diminish, but only slightly as the main cause of UTLS ozone increase from WHFCV was OH reduction, not halogen changes. Model processes (including emissions) and resolution are sources of uncertainty, particularly for parameters in Table S2 with changes $<1\%$. However, because of the large emission and ambient reductions due to WHFCV over current FFOV, it appears safe to conclude that WHFCV will not adversely affect tropospheric pollution or the stratospheric ozone layer. A short-term sensitivity test run with 10% instead of 3% H_2 leakage supports this conclusion.

5. Conclusion

[18] Converting the world's onroad vehicle fleet to wind-powered hydrogen fuel cell vehicles should not change hydrogen or water vapor emissions significantly on a global scale (assuming 3% H_2 leakage with WHFCV), but should reduce emissions and tropospheric levels of many pollutant gases and particles. For example, emission reductions were calculated, over 10 years, to reduce tropospheric CO $\sim 5\%$, CO_2 $\sim 0.55\%$, NO_x ~ 5 –13%, aldehydes ~ 3 –6%, aromatics ~ 5 –15%, PAN $\sim 13\%$, and most other organic gases ~ 3 –15%. Emission reductions also reduced lower- and mid-tropospheric ozone by $\sim 6\%$ but increased column ozone by $\sim 0.41\%$ by increasing UTLS ozone. The increase in UTLS ozone is attributed primarily to a decrease in OH of $\sim 4\%$ caused by decreases in NO_x and aldehydes. The OH reduction in the troposphere increased tropospheric CH_4 by about 0.25%. WHFCV reduced nitric acid and sulfuric acid aerosol and cloud acidification, reduced aerosol

surface area, and increased precipitation, all of which contributed to higher UTLS ozone. Conversion to renewable-powered battery-electric vehicles, which also have near-zero emissions, should have similar impacts as converting to WHFCV.

[19] **Acknowledgments.** Support for this project came from Stanford University's Global Climate and Energy Project, NASA under grants NNG04GJ89G and NNG04GE93G, and the EPA under RD-83337101-O. Partial support came from the DOE under DE-FG36-07GO17108. I would like to thank Cristina L. Archer, John Ten Hoeve, and Mark W. Govett for providing some data.

References

- Barnes, D. H., S. C. Wofsy, B. P. Fehrlau, E. W. Gottlieb, J. W. Elkins, G. S. Dutton, and P. C. Novelli (2003), Hydrogen in the atmosphere: Observations above a forest canopy in a polluted environment, *J. Geophys. Res.*, **108**(D6), 4197, doi:10.1029/2001JD001199.
- Colella, W. C., M. Z. Jacobson, and D. M. Golden (2005), Switching to a U.S. hydrogen fuel cell vehicle fleet: The resultant change in emissions, energy use, and greenhouse gases, *J. Power Sources*, **150**, 150–181.
- Forecast Systems Laboratory (2008), Recent worldwide RAOB observations [CD-ROM], Earth Syst. Res. Lab., NOAA, Boulder, Colo. (Available at <http://www.fsl.noaa.gov/data/onlineodb.html>)
- Granier, C., and G. P. Brasseur (2003), The impact of road traffic on global tropospheric ozone, *Geophys. Res. Lett.*, **30**(2), 1086, doi:10.1029/2002GL015972.
- Jacobson, M. Z. (2001), GATOR-GCMM: 2. A study of daytime and nighttime ozone layers aloft, ozone in national parks, and weather during the SARMAP field campaign, *J. Geophys. Res.*, **106**, 5403–5420.
- Jacobson, M. Z. (2006), Effects of absorption by soot inclusions within clouds and precipitation on global climate, *J. Phys. Chem.*, **110**, 6860–6873.
- Jacobson, M. Z., W. C. Colella, and D. M. Golden (2005), Cleaning the air and improving health with hydrogen fuel cell vehicles, *Science*, **308**, 1901–1905.
- Jacobson, M. Z., Y. J. Kaufman, and Y. Rudich (2007), Examining feed-backs of aerosols to urban climate with a model that treats 3-D clouds with aerosol inclusions, *J. Geophys. Res.*, **112**, D24205, doi:10.1029/2007JD008922.
- Koren, I., Y. J. Kaufman, D. Rosenfeld, L. A. Remer, and Y. Rudich (2005), Aerosol invigoration and restructuring of Atlantic convective clouds, *Geophys. Res. Lett.*, **32**, L14828, doi:10.1029/2005GL023187.
- Logan, J. A. (1999), An analysis of ozonesonde data for the lower stratosphere: Recommendations for testing models, *J. Geophys. Res.*, **104**, 16,151–16,170.
- Schultz, M. G., T. Diehl, G. P. Brasseur, and W. Zittel (2003), Air pollution and climate-forcing impacts of a global hydrogen economy, *Science*, **302**, 624–627.
- Tromp, T. K., R.-L. Shia, M. Allen, J. M. Eiler, and Y. L. Yung (2003), Potential environmental impact of a hydrogen economy on the stratosphere, *Science*, **300**, 1740–1742.
- Warwick, N. J., S. Bekki, E. G. Nisbet, and J. A. Pyle (2004), Impact of a hydrogen economy on the stratosphere and troposphere studied in a 2-D model, *Geophys. Res. Lett.*, **31**, L05107, doi:10.1029/2003GL019224.

M. Z. Jacobson, Department of Civil and Environmental Engineering, Stanford University, Stanford, CA 94305-4020, USA. (jacobson@stanford.edu)